Chalcogenide Letters Vol. 13, No. 2, February 2016, p. 63 - 72

THERMAL TRANSFORMATION AND STRUCTURAL ON $Se_{90}Te_7Cu_3$ CHALCOGENIDE GLASS

F. M. ABDEL-RAHIM[a,b*]

[a] *Physics Department, Faculty of Science and Arts, P.O. Box 355, Code 21921 Khulais, University of Jeddah (UJ), Saudi Arabia.*
[b] *Physics Department, Faculty of Science, Al-Azhar University, P.O. 71452, Assiut Branch, Assiut, Egypt.*

In this study, $Se_{90}Te_7Cu_3$ chalcogenide glass were prepared using the melt quenching technique. The structure and kinetics of the crystallization reaction of amorphous composition were studied under nonisothermal conditions using scanning electron microscopy (SEM) and differential scanning calorimetry (DSC). The characteristic temperatures of the studied chalcogenide glasses has been used to various thermal stability parameters (ΔT, H_R, H_W and S). From the heating rates dependence of values of T_g and T_p, the glass activation energy, E_g, the crystallization activation energy, E_c, the crystallization reaction rate constant K_p and the frequency factor K_0 are derived. The average value of the Avrami exponent comes out to be 1.18, indicating that, the crystallization process takes place via one-dimensional growth with surface crystallization.

(Received December 21, 2015; Accepted February 8, 2016)

Keywords: chalcogenides, heat treatment, DSC, SEM, glass transition, thermal analysis.

1. Introduction

Studying amorphous solids is one of the most active fields of research in the physics of materials science today. Chalcogenide glasses have drawn great attention because of their use in various solid-state devices. One reason for this increase in interest lies in the fact that some amorphous substances show certain unusual switching properties, which could be important in modern technology applications such as switching, electrophotography and memory devices [1-5]. Phase-change memory (PCME, PRAM, PCRAM, Ovonic Unified Memory, Chalcogenide RAM and C-RAM) is a type of non-volatile computer memory. PRAMs exploit the unique behavior of chalcogenide glasses [6-9]. Moreover, addition of a third element such as Cu to binary chalcogenide glass produces a higher stability [10-12].

Study of the crystallization kinetics in amorphous materials has been widely discussed in the literature [13-15]. The determination of kinetic parameters of the crystallization kinetics in chalcogenide glasses using differential scanning calorimetric (DSC) technique is a very common procedure. The data is normally analyzed using different theoretical models [16, 17].

In the present work, the crystallization kinetics of amorphous $Se_{90}Te_7Cu_3$ is investigated by non-isothermal DSC. Different models were used to extract the kinetic parameters of the transformation. On the light of the present data, the nucleation and growth mechanisms operating during the crystallization were suggested.

---

[*] Corresponding author: farid.elkhateb@gmail.com

2. Experimental

Bulk of $Se_{90}Te_7Cu_3$ chalcogenide glasses by synthesizing the initial materials (Se, Te and Cu) of 5 N purity in evacuated (10^3 Pa) quartz ampoules in a furnace. The blends of Se, Te and Cu weighing about 5 g were heated at 2–5 K/min to about 1373 K and kept at this temperature for 2–3 h. During the melt process, the tube was frequently shaken to homogenize the resulting alloy. The melt was quenched in ice water to obtain the material in glassy state.

For the scanning electron microscopy (SEM) examinations, sample surfaces were etched using concentrated HNO_3. The etching time was usually 20 s. After that, the surface was ultrasonically cleaned in alcohol. The surface morphology measurements were investigated for glasses using JEOL JSM-6360LV, Japan, scanning electron microscope (SEM) operated at an accelerating voltage of 15 kV with 10 mm work distance. The composition and Surface morphology were studied using Scanning electron microscope (SEM) of make Phillips XL30 ESEM operated at 20 kV with energy dispersive X-ray analysis (EDAX) attachment operated at 20 kV with detector SUTW- Sapphire and tilt ~0.3–0.7°.

The thermal behavior was investigated using a Shimadzu DSC-50. Typically, 20 mg of sample in powder form was sealed in standard aluminum pans and heated at different rates ranging from 5 to 50 K/min. The accuracy of the heat flow is $\pm 10^{-3}$ W/m and the temperature precision as determined by the microprocessor of the thermal analyzer is ± 0.1 K. The crystallized fraction (χ), at a given temperature (T), is given as $\chi = (A_T/A)$, where A is the total area of the exothermic peak between the onset temperature (T) where crystallization just begins and the temperature (T_f) where the crystallization is completed and A_T is the area between T_0 and T. A best fit for the results was calculated by the least-square method. The arithmetic means as well as the standard deviation were obtained for the activation energies.

3. Results and discussions

3.1 Structural study

Qualitative and quantitative calculations were performed using the EDX technique accomplished with SEM from the displayed characteristic X-ray pattern. The results obtained are shown in Fig. 1. The atomic percentage ratios of Se, Te and Cu were found to be 89.97, 7.01 and 3.02, respectively.

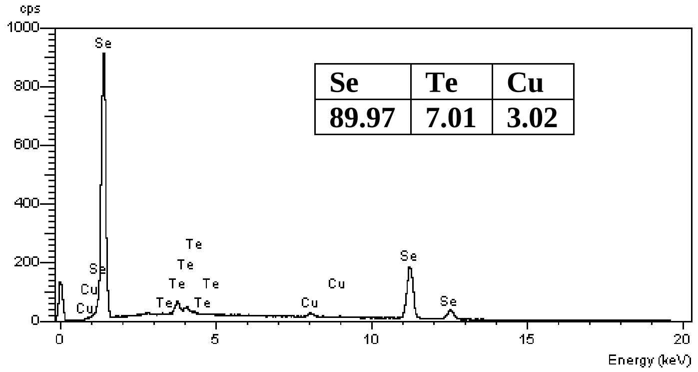

Fig. 1: EDX spectrum of $Se_{90}Te_7Cu_3$ glass

By using SEM to recorded the change in morphology under isothermal annealing. The morphology of $Se_{90}Te_7Cu_3$ recovered for the as prepared bulk specimen is shown in Fig. 2a. The micrograph shows the conchoidal contours, which indicate the glassy state. Fig. 2b–d show the effect of heat treatment on the $Se_{90}Te_7Cu_3$ chalcogenide under nitrogen flow. Fig. 2b shows an SEM micrograph of $Se_{90}Te_7Cu_3$ sample after annealing for 15 min at 350 K. The micrograph indicates that the glass structure is still unchanged, but with some distortion. This distortion dramatically increases as temperature increases, accompanied by the beginning of crystallization as shown in Fig. 2c for a sample annealed at 370 K for 30 min. By increasing the annealing temperature to 390 K for 15 min, the crystalline morphology covered the specimen surface and extended into the bulk material as shown in Fig. 2d. The crystalline morphology is homogenous and covers the specimen surface completely.

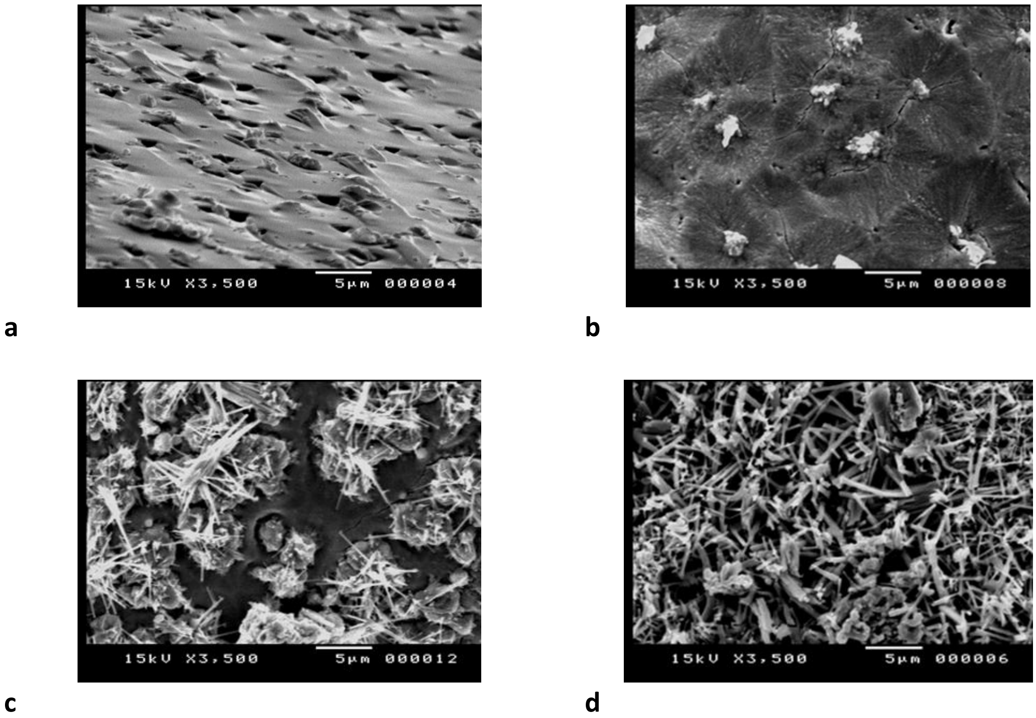

Fig. 2: SEM micrograph of $Se_{90}Te_7Cu_3$ annealed for 30 min at different temperature: (a) as quenched in bulk specimen x *3500; (b) annealed at 350 K,* x *3500; (c) annealed at 370 K,* x *3500; (d) annealed at 390 K,* x *3500.*

A typical DSC curve of the bulk $Se_{90}Te_7Cu_3$ glass in powdered form, using a Shimadzu DSC-50 differential scanning calorimetry at a heating rate of 10 K/min, is shown in Fig.3a. Three characteristic phenomena are clear in the studied temperature range. The first one (T_g= 326.22 K) corresponds to the glass transition temperature, the second one (T_c= 360.29 K) to the onset temperature of crystallization, the third one to the peak temperature of crystallization (T_p=400.59 K) and the last one to the melting temperature (T_m=502.35 K). The slight shoulder p appeared in the left-hand side of the exothermic peak means that more than one crystalline phase are growing during the DSC run. This behavior is typical for glass-crystalline transformation. Fig. 3b shows a set of DSC thermograms of $Se_{90}Te_7Cu_3$ glass at different heating rates (α). Values of the characteristic temperature (T_g, T_c, T_p, and T_m) and the stability criterion parameters (ΔT, H_R , H_W and S) based on these characteristic temperature for $Se_{90}Te_7Cu_3$ chalcogenide glasses are listed in Table 1.

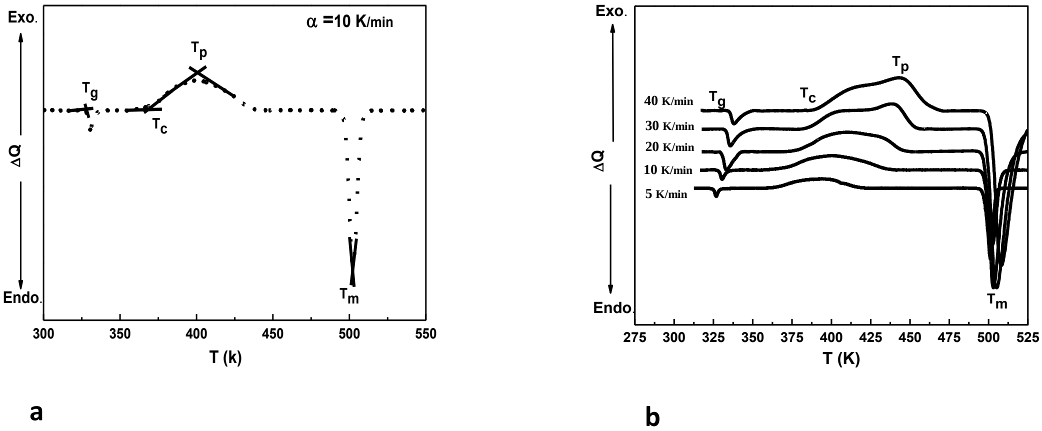

Fig. 3: (a) Typical DSC trace of $Se_{90}Te_7Cu_3$ glass at heating rate of 10 K/min and (b) DSC trace of $Se_{90}Te_7Cu_3$ glass at different heating rates

Table 1:Values of the characteristic temperature (T_g, T_c, T_p, and T_m) and the stability criterion parameters (ΔT, H_R H_W and S) based on these characteristic temperature for $Se_{90}Te_7Cu_3$ chalcogenide glasses.

Heating rates (α) (K/min)	T_g (K)	T_c (K)	T_p (K)	T_m (K)	ΔT (K)	H_R	H_W	S (K)
5	321.91	359.33	393.87	501.05	37.42	0.26404	0.11624	4.01506
10	326.22	360.29	400.59	502.35	34.07	0.27575	0.1167	4.23622
20	329.10	369.40	410.19	503.07	40.30	0.30149	0.12246	4.99495
30	331.02	381.40	438.01	504.94	50.38	0.41169	0.15387	8.71055
40	332.54	384.28	439.93	505.05	53.74	0.44100	0.1609	8.9539

3.2 The activation energy of glass transition (Eg):

Two approaches are used to analyze the dependence of T_g on the heating rate, α, [18]. One is the empirical relationship of the form:

$$T_g = A + B\ln(\alpha) \tag{1}$$

where A and B are constants for a given glass composition. This equation was suggested by Lasocka [19]. The results of Fig. 4 show the validity of this relationship for $Se_{90}Te_7Cu_3$ glass. For this glass, the empirical formula can be rewritten in the form:

$$T_g = 313.54 + 4.32\ln(\alpha) \tag{2}$$

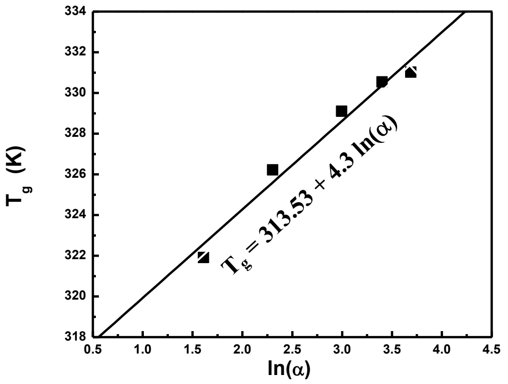

Fig. 4: T_g *versus* $\ln(\alpha)$ *for* $Se_{90}Te_7Cu_3$ *chalcogenide glasses.*

The second approach using Kissinger's formula [20, 21], the dependence of the glass transition temperature on the heating rate, α, was found to obey the following equation [22,23]

$$\ln\left(\alpha/T_g^2\right) = -E_g/\left(RT_g\right) + Const. \quad (3)$$

where E_g is the glass transition activation energy. Plots of $\ln\left(\alpha/T_g^2\right)$ versus $(1/T_g)$ for $Se_{90}Te_7Cu_3$ glass give a linear behavior up to heating rate of 40 K/min. The variation in $\ln\left(1/T_g^2\right)$ with $\ln(\alpha)$ is much slower than $(1/T_g)$ with $\ln(\alpha)$ [19, 24–26]. The Kissinger equation can be simplified to

$$\ln(\alpha) = -E/\left(RT_g\right) + Const. \quad (4)$$

The variation of $\ln\left(\alpha/T_g^2\right)$versus $(1/T_g)$ and $\ln(\alpha)$ versus $(1/T_g)$ for $Se_{90}Te_7Cu_3$ glass are shown in Fig. 5.

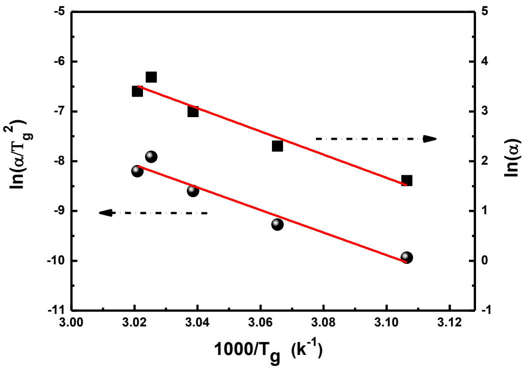

Fig. 5: $\ln(\alpha/T_g^{2})$ *and* $\ln(\alpha)$ *versus* $(1000/T_g)$ *for* $Se_{90}Te_7Cu_3$ *chalcogenide glasses.*

The value of E_g deduced from relation (3) is 188.31±3 kJ/mol and its value calculated from Eq. (4) is 193.79±3 kJ/mol. From the values of E_g, one can use both relations (3) and (4) to evaluate the glass transition activation energy for $Se_{90}Te_7Cu_3$ glass. The average value of E_g is 191.05±3 kJ/mol as shown in Table 2.

Table 2:Values of the activation energy for glass transition (E_g) and the activation energy for crystallization (E_c) deduced from different methods and values of (ln K_o, n and K_p) for $Se_{90}Te_7Cu_3$ chalcogenide glasses.

Name of method	**E_g (KJ/mol)**		**E_c (KJ/mol)**					**ln K_0**	**n**	**K_p**
	Kissinger Eq. (3)	**Moynihan Eq. (4)**	**Kissinger Eq. (5)**	**Mahadevan Eq. (6)**	**Matusita Eq. (7)**	**Gao & Wong Eq. (8)**	**Augis & Bennett Eq. (10)**			
	193.79±3	188.31±3	198.15±5.5	227.10±4.5	248.53±4.3	137.23±3.4	212.43±5.8	**11.4±3.2**	1.19 at (422K) 1.12 at (417K) 1.24 at (410K)	**3.2**
Average values	**191.05±3**		**221.13±4.95**						**1.18**	

3.3 The activation energy for crystallization (E_c):

Kissinger method has been also applied in the analysis of the exothermic peak to get the activation energy for crystallization using the following equation:

$$\ln\left(\alpha/T_p^2\right) = -E_c/\left(RT_p\right) + Const. \tag{5}$$

When the variation of 1000/T_p^2 with ln α is much slower than that of 1000/T_p with ln α, Mahadevan et al. [29] have approximated Eq. (5) to the following form:

$$\ln\alpha = -E_c/\left(RT_p\right) + Const. \tag{6}$$

Fig. 6 shows the plot of $\ln\left(\alpha/T_p^2\right)$ and ln α versus (1000/T_p) for all heating rates for the two studied compositions. All curves are linear and from the slopes of the straight lines, the activation energies can be evaluated and the values of (E_c) are 198.15±5.5 and 227.10±4.5 kJ/mol.

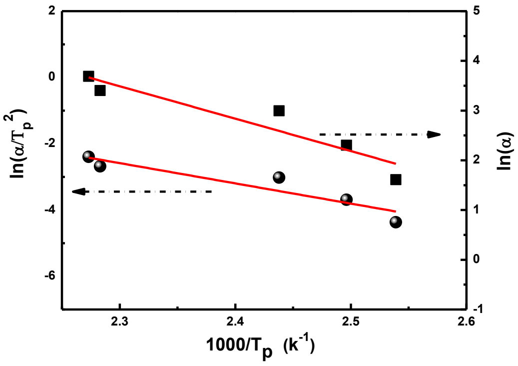

Fig. 6: $\ln(\alpha/T_p^2)$ and $\ln(\alpha)$ versus ($1000/T_p$) for $Se_{90}Te_7Cu_3$ chalcogenide glasses

An attempt has also been made to calculate the activation energies of $Se_{90}Te_7Cu_3$ samples using the Matusita formulation [30]:

$$\ln\left(-\ln\left(1-x\right)\right) = -n\ln\left(\alpha\right) + 1.052m\,E_c/RT_p + Const. \tag{7}$$

where x is the crystallized volume fraction while n and m are related to the dimensionality and mechanism of growth. Fig. 7 depicts the relationship between the crystallized volume fraction (x)

and temperature for $Se_{90}Te_7Cu_3$ chalcogenide glasses at different heating rates. Based on this figure, we can obtain plots of ln[-ln(1- x)] against ln α at three fixed temperatures, as shown in Fig. 8. From the slope of this relation, the order of the crystallization mechanism n (Avrami index) can be obtained and its mean values were found to be 1.18 for $Se_{90}Te_7Cu_3$. For as-quenched glass which does not contain any nuclei n = m+1, while for a glass contains a sufficiently large number of nuclei n = m. It is observed that all the glassy materials predominantly crystallize in one dimensions suggesting surface nucleation.

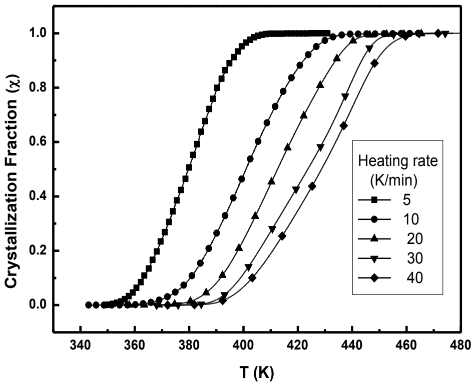

Fig. 7: The crystallization fraction (χ) versus Temperature (K) for $Se_{90}Te_7Cu_3$ chalcogenide glasses at different temperature.

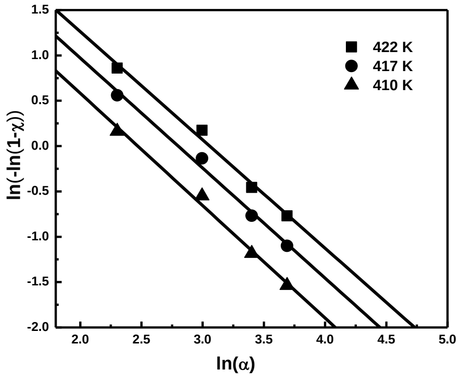

Fig. 8: ln(-ln(1-x)) versus ln(α) for $Se_{90}Te_7Cu_3$ chalcogenide glasses at different temperature.

On the other hand, the activation energy for crystallization (E_c), has also been calculated from Matusita equation. The plot of ln[-ln(1- x)] versus 1000/T at all heating rates as shown in Fig. 9, yields a straight line, the slope of this line gives the activation energy for crystallization (E_c) and its value equals 248.53±4.3 kJ/mol.

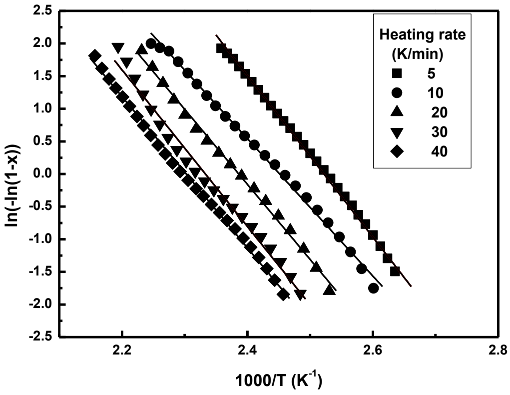

Fig. 9: ln(-ln(1-x)) versus (1000/T) for $Se_{90}Te_7Cu_3$ *chalcogenide glasses.*

Furthermore, Gao and Wang [31] have proposed a slightly different method to analyze DSC thermograms in terms of thermal parameters, during the crystallization process. The theoretical idea is based on the same fundamental assumptions imposed on the JMA transformation equation. It assumes that the nucleation is randomly distributed, and that the growth rate of the new phase depends on the temperature but not on time. The theory provides the relationship between the maximum crystallization rate and the peak crystallization temperature in the form:

$$\ln(dx/dt)_p = -E_c/RT_p + const. \tag{8}$$

After differentiation with respect to (1/T), the above equation takes the following form:

$$d\left[\ln(dx/dt)_p\right]/d\left(1/T_p\right) = -E_c/R \tag{9}$$

where (d*x*/dt) is the rate of volume fraction crystallized at the peak of crystallization, which is proportional to the peak height. The activation energy of the amorphous–crystalline transformation (E_c) and the frequency factor K_0 where calculated using the method proposed by Augis and Bennett:

$$\ln\left(\alpha/T_p\right) = -E_c/\left(RT_p\right) + \ln K_0 \tag{10}$$

Fig. 10 shows the plot of ln(d*x*/dt) and $\ln\left(\alpha/T_p\right)$ versus 1000/T_p and the activation energy is determined from the slope of the straight lines and gives the values of 137.23±3.4 and 212.43±5.8kJ/mol respectively for $Se_{90}Te_7Cu_3$.

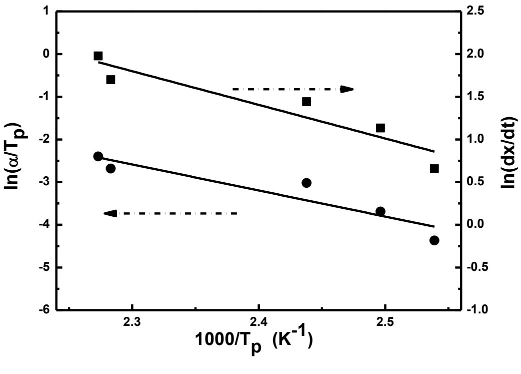

Fig. 10: ln(α/T$_p$) and ln(dx/dt) versus (1000/T) for $Se_{90}Te_7Cu_3$ *chalcogenide glasses.*

The crystallization reaction rate constant (K_p) corresponding to the temperature at which the crystallization rate is maximum were calculated from the thermodiagrams by using equation:

$$\alpha E_c / RT_p K_p = 1 \tag{11}$$

The difference in the activation energy as calculated with the different models may be attributed to different approximations used in the models. The activation energies (E_c) and values (ln K_0, n *and* K_p) of the sample calculated by means of the different theoretical models are summarized in Table 2.

Kissinger's equation was basically developed for studying the variation of the peak crystallization temperature with heating rate. According to Kissinger's method, the transformation under non-isothermal condition is represented by a first order reaction. Matusita and Sakka [30] have developed a method on the basis of the fact that, crystallization does not advance by an *n*-order reaction but by a nucleation and growth process. They emphasized that, the crystallization mechanisms such as bulk crystallization (bulk nucleation followed by two- or three-dimensional growth) or surface crystallization (bulk nucleation followed by linear growth) should be taken into account for obtaining E_c. In addition to the activation energy, Matusita's method provides information about the Avrami exponent and the dimensionality of growth. The model developed by Gao and Wang for the calculation of the kinetic parameters is preferred over all the other three models because of its dependency on the heating rate and temperature and it gives us the average values.

Conclusions

The structure and kinetics of crystallization of $Se_{90}Te_7Cu_3$ were investigated. The morphology of specimens annealed at selected stages of heat treatments for 15 min showed different crystalline structures.

The average value of the activation energy of the glass transition (E_g) is 191.05±3 kJ=mol. The average value of the activation energy for crystallization E_c of the investigated glass using different methods is 221.13±4.95 kJ/mol. One crystallization mechanism, one-dimensional growth, is working during the amorphous–crystalline transformation. Values of the crystallization reaction rate constant (K_p) and the frequency factor (K_0) are calculated by using the methods proposed.

References

[1] R. Chiba, N. Funakoshi, J. Non-Cryst. Solids **105**, 149 (1988).
[2] M. Mehdi, G. Brun, J.C. Tedenac, J. Mater. Sci. **30**, 5259 (1995).
[3] S.R. Elliott, Physics of Amorphous Materials, 2nd ed., Longman Scientific & Technical, Essex, UK, 1990.
[4] Z. Ogorelec, A. Tonejc, Mater. Lett. **42**, 81 (2000).
[5] B. Bureau, J. Troles, M. Le Floch, F. Smektala, J. Lucas, J. Non-Cryst. Solids **326**, 58 (2003).
[6] T. Ohta, J. Optoelectron. Adv. Mater. **3**, 609 (2001).
[7] A.K. Kolobov, J. Tominaga, J. Optoelectron. Adv. Mater. **4**, 679 (2002).
[8] D. Lezal, J. Optoelectron. Adv. Mater. **5**, 23 (2003).
[9] A.N. Upadhyay, R.S. Tiwari, Kedar Singh, Materials Letters, Accepted date (2015)31 October.
[10] M. Mehdi, G. Brun, J.C. Tedenac, J. Mater. Sci. **30**, 5259 (1995).
[11] M. Kastner, Phys. Rev. Lett. **28**, 355 (1972).
[12] R.M. Mehra, R. Kumar, P.C. Mathur, Thin Solid Films **170**, 15 (1989).
[13] N. Afify, J. Non-Cryst. Solids **128**, 279 (1991).
[14] H. Yinnon, D.R. Uhlmann, J. Non-Cryst. Solids **54**, 253 (1983).
[15] A.H. Moharram, M.S. Rasheedy, Phys. Stat. Sol. A **169**, 33 (1998).

[16] A.A. Abu-Sehly1, A.A. Elabbar, Physica B **390**, 196 (2007).
[17] Farid M. Abdel-Rahim, K. A. Aly, Journal of Non-Crystalline Solids **419**, 69 (2015).
[18] A.B. Abdel El-Moiz, N. Afify, M.M Hafiz, Physica B **182**, 33 (1992).
[19] M. Lasocka, Mater. Sci. Engng **23**, 173 (1976).
[20] H.E. Kissinger, J. Res. Nat. Bur. Stand. **57**, 217 (1956).
[21] H.E. Kissinger, Anal. Chem. **29**, 1702 (1957).
[22] H.S. Chen, J. Non-Cryst. Solids **27**, 257 (1978).
[23] J.A. Macmillan, J. Phys. Chem. **42**, 3497 (1965).
[24] M.M. Hafiz, N. Afify, M.A Osman, M. Dongol, J. Thermal Anal. **36**, 2417 (1990).
[25] N. Afify, A.H. Moharram, M Dongol, M.M. Hafiz, Physica B **176**, 301 (1992).
[26] A. El-Korashy, N. Afify, J. Thermal Anal. **37**, 507 (1991).
[27] A.H. Moharram, A.A. Abu-Sehly, M. Abu El-Oyoun, A.S. Soltan, Physica B **324**, 344 (2004).
[28] A.H. Moharram, M. Abu El-Oyoun, J. Phys. D **33**, 700 (2000).
[29] S. Mahadevan, A. Giridhar, A.K. Singh, J. Non-Cryst. Solids **81**, 11 (1986).
[30] K. Matusita, S. Sakka, Phys. Chem. Glasses **20**, 81 (1979).
[31] Y.Q. Gao, W. Wang, J. Non-Cryst. Solids **81**, 129 (1986).